Computational and Structural Biotechnology Journal 21 (2023) 2960–2972

Contents lists available at ScienceDirect

Computational and Structural Biotechnology Journal

journal homepage: www.elsevier.com/locate/csbj

Discovery and analysis of a novel antimicrobial peptide B1AW from the skin secretion of *Amolops wuyiensis* and improving the membrane-binding affinity through the construction of the lysine-introduced analogue

Haixin Qin [a,b,c], Weimin Zuo [a,b,c], Lilin Ge [d], Shirley W.I. Siu [e], Lei Wang [f], Xiaoling Chen [f], Chengbang Ma [f], Tianbao Chen [f], Mei Zhou [f,*], Zhijian Cao [g,*], Hang Fai Kwok [a,b,c,**]

[a] Institute of Translational Medicine, Faculty of Health Sciences, University of Macau, Avenida da Universidade, Taipa, Macau
[b] Department of Biomedical Sciences, Faculty of Health Sciences, University of Macau, Avenida da Universidade, Taipa, Macau
[c] MoE Frontiers Science Center for Precision Oncology, University of Macau, Avenida da Universidade, Taipa, Macau
[d] College of Pharmacy, Nanjing University of Chinese Medicine, Nanjing 210023, China
[e] Institute of Science and Environment, University of Saint Joseph, Estrada Marginal da Ilha Verde, Macau
[f] School of Pharmacy, Queen's University Belfast, 97 Lisburn Road, Belfast BT9 7BL, UK
[g] State Key Laboratory of Virology and Modern Virology Research Center, College of Life Sciences, Wuhan University, Wuhan 430072, China

ARTICLE INFO

Article history:
Received 13 March 2023
Received in revised form 4 May 2023
Accepted 4 May 2023
Available online 6 May 2023

Keywords:
Brevinin peptide
Peptide modification
Antimicrobial peptide
Anticancer peptide
Molecular dynamic simulation

ABSTRACT

In the development and study of antimicrobial peptides (AMPs), researchers have kept a watchful eye on peptides from the brevinin family because of their extensive antimicrobial activities and anticancer potency. In this study, a novel brevinin peptide was isolated from the skin secretions of the Wuyi torrent frog, *Amolops wuyiensis* (*A. wuyiensisi*), named B1AW (FLPLLAGLAANFLPQIICKIARKC). B1AW displayed antibacterial activity against Gram-positive bacteria *Staphylococcus aureus* (*S. aureus*), methicillin-resistant *Staphylococcus aureus* (*MRSA*), and *Enterococcus faecalis* (*E. faecalis*). B1AW-K was designed to broaden the antimicrobial spectrum of B1AW. The introduction of a lysine residue generated an AMP with enhanced broad-spectrum antibacterial activity. It also displayed the ability to inhibit the growth of human prostatic cancer PC-3, non-small lung cancer H838, and glioblastoma cancer U251MG cell lines. In molecular dynamic (MD) simulations, B1AW-K had a faster approach and adsorption to the anionic membrane than B1AW. Therefore, B1AW-K was considered a drug prototype with a dual effect, which deserves further clinical investigation and validation.

1. Introduction

Amphibian skin secretions have long been established as an abundant source of bioactive compounds [1]. Chansu, a powerful drug secreted from the skin of toads used in a traditional Chinese medicine, may be considered an example. In ancient times, the Chinese found Chansu exhibited excellent anti-inflammatory, analgesic, and anti-diarrhoeic, and anti-emetic properties [2,3]. In recent years, many scientists have conducted in-depth studies on the complex functional components of amphibian skin secretions. Antimicrobial peptides (AMPs) are important bioactive components in the skin secretions of many frogs [4].

Although antibiotics are one of the most successful drug discoveries in human medical history, the rapid development of antibiotic resistance has limited their future application in recent years [5]. AMPs, as alternative antimicrobial agents may potentially solve the problem of antibiotic resistance, and thus have attracted the attention of scientists. Currently, AMPs are being studied extensively. As part of the innate defence system, most AMPs have broad-spectrum antimicrobial activity [6,7]. The cationic AMPs interact with the negatively charged membrane of microorganisms through electrostatic interactions, leading to cell death through Carpet, Barrel-Stave

* Corresponding authors.
** Corresponding author at: Institute of Translational Medicine, Faculty of Health Sciences, University of Macau, Avenida da Universidade, Taipa, Macau.
E-mail addresses: m.zhou@qub.ac.uk (M. Zhou), zjcao@whu.edu.cn (Z. Cao), hfkwok@um.edu.mo (H.F. Kwok).

https://doi.org/10.1016/j.csbj.2023.05.006

and/or Toroidal Pore modes[8]. This mechanism of action differs from that of traditional antibiotics. AMPs can bind to the cell membrane on multiple targets and can kill cells in a short time due to their target location on the surface of the cell membrane [9], which means there is a low possibility that AMPs induce drug resistance [10]. However, the membrane target of AMPs makes their selectivity low. AMPs can attack host cells, resulting in cytotoxicity and haemolytic activity [11]. Thus, the balance between bioactivity and toxicity of AMPs is an important index that must be considered [4].

Among the known AMPs of amphibian origin, brevinin-1 peptides are among the most common, belonging to the brevinin superfamily [12]. Since the first brevinin peptide was discovered in 1992, almost 985 types of brevinins have been isolated [13,14]. Generally, brevinin-1 family peptides share some typical characteristics, including a high hydrophobic 'FLP' motif at the N-terminus and a 'Rana box' (Cys^{18}-X * 4–Lys^{23}-Cys^{24}, where X can be any amino acid) located at the C-terminus [12,15]. Based on their hydrophobicity and cationicity, brevinin-1 peptides have been shown to exhibit various bioactivities against bacteria, fungi, and different human cancer cell lines [15–17].

In this study, we identified a novel brevinin peptide from cascade of frog skin secretions, *Amolops wuyiensis*, named B1AW. Shotgun cloning was used to determine the full sequence of this peptide through cloning of its precursor cDNA. B1AW displayed potent antimicrobial activities against three Gram-positive bacteria and an excellent inhibitory effect towards three human cancer cell lines. Unlike other brevinins, the narrow antimicrobial spectrum limited the further application of B1AW. To optimise its bioactivity, we constructed a modified peptide with an additional lysine residue. The long and positively charged side chain featuring the lysine residue improves the permeability of the peptide across the microbial membrane and also promotes the binding affinity of AMPs to the negatively charged phospholipid layer [18,19]. By introducing a lysine residue, the B1AW-K modification achieved broad-spectrum antimicrobial activities and enhanced antiproliferative effects against human cancer cell lines. Furthermore, through a series of molecular dynamic (MD) simulations, B1AW-K was found to have higher selectivity toward the anionic cell membrane. This study provides a theoretical basis for optimising AMPs through rational design.

2. Materials and Methods

2.1. Skin secretion harvesting from Amolops wuyiensis

Adult samples of *Amolops wuyiensis* were supplied from a commercial source in the United Kingdom. Before starting the experiment, the frogs were fed on a day/night cycle (12 h/12 h) in a specialised tropical amphibian facility at Queen's University Belfast at a constant temperature of 25 °C for at least 4 weeks. Then electrical stimulation (5 V, 100 Hz, 140 ms width) through platinum electrodes for 20 s. Five frog samples were used to obtain the dorsal skin secretions [20]. Deionised water was used to rinse the skin secretions from the skin into a chilled beaker. The skin secretions were then snap frozen in liquid nitrogen and lyophilised. The lyophilised samples were stored at − 20 °C for further analysis. The study was performed in accordance with the guidelines of the UK Animal (Scientific Procedures) Act 1986, project licence PPL 2694, issued by the Department of Health, Social Services and Public Safety, Northern Ireland. The procedures were reviewed by the Institutional Animal Care and Use Committee (IACUC) of Queen's University Belfast and approved on 1 March 2011.

2.2. Identification of precursor-encoding cDNAs (complementary DNA) from skin secretion

Poly-A mRNA was extracted using the Dynabeads mRNA Direct kit (Dynal Biotech, Merseyside, UK) because of covalent pairing and was synthesised into a first-strand cDNA library. A SMART-RACE kit (Clontech, Mountain view, Califronia, USA) and a degenerate sense primer were then used to conduct the RACE-PCR (Rapid amplification of cDNA ends-Polymerase chain reaction) process so mRNA could be obtained. The PCR products were purified and cloned. The cloned products then sequenced as described in a previous study [21]. The National Centre for Biotechnology Information (NCBI) database was used to analyse the similarity between B1AW and other reported peptides.

2.3. Synthesis and purification of peptides

Two-Channel Tribute Peptide Synthesiser (Protein Technologies, Tucson, Arizona, USA) was used to synthesis the novel peptide B1AW and its analogues, using the solid phase 9-fluorenyl methoxycarbonyl (Fomc) chemistry strategy. After synthesis, the crude products were purified by reverse phase HPLC (Phenomenex Aeris PEPTIDE 5 μm XB-C18 column, 250 × 21.2 mm, Hong Kong, China) with a linear gradient formed from 80% buffer A (0.05/99.5 (v/v) Trifluoroacetic acid (TFA)/water) and 20% buffer B (0.05/19.95/80.00 (v/v/v) TFA/water/Acetonitrile (ACN)) to 0% buffer A: 100% and buffer B in 60 min at a flow rate of 8 mL/min. The column effluent was continuously monitored at a wavelength of 280 nm. The primary structure of the peptides was confirmed by matrix-assisted laser desorption/ionisation-time of flight mass spectrometry (MALDI-TOF MS) (Voyager DE, Perspective Biosystem, Foster City, California, USA) in positive detection mode usingα-cyano-4-hydroxycinnamic acid (CHCA) as the matrix. The purified peptides were subjected to lyophilisation and stored at − 20 °C.

2.4. Physicochemical properties and secondary structure analysis

The chemical structures of B1AW and its analogue were generated by the online web server (https://www.allpeptide.com/jiegoutu.html; Accessed: 2023/04/20). The physicochemical properties of B1AW and its analogue were determined through the Heliquest site (http://heliquest.ipmc.cnrs.fr/cgi-bin/ComputParamsV2.py; Accessed: 2023/02/21). The three-dimensional (3D) model construction and α-helicity potential of each amino acid were evaluated by the PEP-FOLD server [22].

Circular dichroism (CD) analysis was used to determine the secondary structure of the synthesised peptides, and was performed on a JASCO J815 Spectropolarimeter (JASCO Inc., Easton, Maryland, USA). The peptide samples were dissolved in 50% trifluoroethanol (TFE)/10 mM ammonium acetate buffer (NH_4Ac) and 10 mM NH_4Ac to reach a final concentration of 100 μM and then loaded into a 1-mm path length cuvette (Hellma Analytics, Essex, UK). CD spectra were measured in the range of 190–250 nm at 20 °C at a scanning speed of 200 nm/min with a 1-nm bandwidth and 0.5-nm data pitch. K2D3 (http://cbdm-01.zdv.uni-mainz.de/~andrade/k2d3/; Accessed: 2023/02/21), the online analysis web server, was used to analyse the collected results.

2.5. Evaluation of antimicrobial activity: determination of minimum inhibitory concentration (MIC) and minimum bactericidal concentration (MBC)

Seven different microorganisms were used to screen the antimicrobial activity of B1AW and its analogues. Gram-positive bacteria: *S. aureus* (ATCC 6538), *E. faecalis* (NCTC 12697), and MRSA (NCTC 12493); Gram-negative bacteria: *E. coli* (ATCC 8739),

Pseudomonas aeruginosa (*P. aeruginosa*) (ATCC 9027), and *Klebsiella pneumoniae* (*K. pneumoniae*) (ATCC 43816), and yeast, *Candida albicans* (*C. albicans*) (ATCC 10231). The microorganisms tested were incubated in Muller-Hinton broth (MHB) (for bacteria) or yeast extract peptone dextrose broth (YPD-B) (for yeast) medium at 37 °C overnight in an orbital incubator. After incubation, 500 μL of culture were transferred to a McCartney bottle with 20 mL of fresh prewarmed corresponding medium for subculture until the microorganisms reached their respective logarithmic growth phases (Gram-negative and Gram-positive bacteria: 5×10^5 CFU/mL; yeast: 1×10^6 CFU/mL).

For the MIC assay, subcultured microorganisms were added to 96-well plates and treated with dissolved PBS peptides (to the final concentrations of 1–512 μM), and other control groups were used to treat these suspensions of microorganisms at 37 °C for 24 h. A Synergy HT plate reader (Biotec, Minneapolis, Minnesota, USA) was then used to detect the absorbance of each well at 550 nm. The MIC value represents the lowest concentration of peptides at which there was no visible growth of the microorganism after 24 h of incubation [23]. PBS was used as the negative control, 2 mg/mL norfloxacin and 1 mg/mL amphotericin B were used as the positive control for bacteria and yeast, respectively. Each group had three replicates and the experiment was repeated three times.

After determining MIC values, 10 μL of the medium of each clear well was inoculated on a Mueller–Hinton agar plate (MHA, for bacteria) or yeast extract peptone dextrose agar plate (YPD-A, for yeast) plate and incubated for 24 h for measurement of MBC values. The MBC value was the lowest concentration of a peptide that kills 99.9% of bacteria.

2.6. Evaluation of antibiofilm activity: determination of the minimum biofilm inhibitory concentration (MBIC) and the minimum biofilm eradication concentration (MBEC)

Gram-positive bacteria mentioned in 2.6 were chosen to test the antibiofilm activities of B1AW and B1AW-K; Gram-negative bacteria mentioned in Section 2.6 were used to assess the antibiofilm activity of B1AW-K. The Gram-positive bacteria were cultured in Tryptic Soy Broth (TSB) and the Gram-negative bacteria were cultured in Lysogeny broth (LB). The final concentrations of the peptide solution ranged from 1 μM to 256 μM. Bacteria culture without any treatment served as a growth control, and bacteria culture treated with PBS served as a negative control. Each group had three replicates and the MBIC and MBEC assays were repeated three times.

For the determination of MBIC, bacteria cultures at 1×10^6 CFU/mL were incubated with the tested peptide in a 96-well plate (100 μL/well) for 24 h. Each well was washed with PBS after incubation. Then, 125 μL of methanol (90%, v/v) was added to fix the biofilm and the wells were dried and stained with 125 μL of crystal violet (0.1%, w/v) for 30 min. After staining, excess stain was removed, and the wells were completely dried. Next, the stained biofilm in each well was then dissolved using 150 μL of acetic acid (30%, v/v). After dissolution, the suspension was transferred to a new 96-well plate to detect the absorbance at 595 nm by the Synergy HT plate reader. MBIC was the minimum concentration of the peptide that did not show biofilm formation.

For the MBEC assay, the bacterial culture was removed after the bacteria were cultured in the 96-well plate for 24 h to form the mature biofilm. The biofilm was then further washed with PBS. Then fresh broth containing different concentrations (1–256 μM) was added to the plate for a 24-h incubation at 37 °C. The subsequent steps were consistent with the MBIC assay, as described above.

2.7. Time-killing assays

Due to the relatively similar antimicrobial activity of B1AW and B1AW-K against Gram-positive bacteria, the time-killing kinetic abilities of both peptides against *S. aureus* (ATCC 6538) were tested to select the better peptide for subsequent modifications. The bacteria culture was prepared in the same way as for the MIC assay (described in Section 2.5). After a 24-h incubation and subculture, the bacteria culture (1×10^6 CFU/mL) was mixed with peptide solutions at the respective MIC and 2 × MIC concentrations in sterile 1.5-mL tubes. At time points of 0, 5, 10, 15, 30, 60, 90, 120, and 180 min, 20 μL of the bacteria-peptide mixture was removed from culture tubes and then added to 180 μL of sterile PBS to make a 10-fold dilution. Then, 10 μL of the diluted bacteria-peptide mixture was seeded in MHA plates. The plates were incubated at 37 °C for 24 h before colony counting. The bacteria cultured without any treatment were used as the growth control, and the bacteria culture treated with PBS served as the negative control.

2.8. Bacterial cell membrane permeability assays

S. aureus (ATCC 6538) was chosen to test the permeabilisation effect of B1AW and B1AW-K. *E. coli* (ATCC 8739) were used to test the permeabilisation effect of B1AW-K. *S. aureus* (ATCC 6538) and *E. coli* (ATCC 8739) were cultured overnight in TSB and LB, respectively. Next, the growth medium containing bacteria in the logarithmic growth phase was centrifuged at 1000g for 10 min at 4 °C to collect bacterial cells. The cells were washed with 5% TSB or 5% LB in 0.85% NaCl solution twice and resuspended.

A 90-μL volume of bacteria was then incubated with peptide solutions at the respective MIC and 2 × MIC concentrations in a black 96-well plate at 37 °C for 2 h. After incubation, 10 μL of SYTOX™ green nucleic acid stain (50 μM in TSB or LB, Life Technologies, Cheshire, UK) was added to each well and incubated for 5 min in the dark at 37 °C. A Synergy HT plate reader (Biotech, Minneapolis, Minnesota, USA) was used to measure the fluorescent intensity with an excitation wavelength of 484 nm and an emission wavelength of 528 nm. Negative controls: bacteria treated with 5% TSB or LB medium; positive control: bacteria treated with 70% (v/v) isopropanol for 1 h; blank controls: 5% TSB or LB medium without bacteria. The permeability rate was measured relative to the positive control groups.

2.9. Assessment of mammalian cell proliferation inhibitory effect — MTT assays

In these assays, human prostate carcinoma cancer cells, PC-3 (ATCC®-CRL-1435TM), human non-small cell lung cancer cells, H838(ATCC®-CRL-5844), human glioblastoma/astrocytoma cancer cells, U251MG (ECACC-09063001), human microvascular endothelial cell line, HMEC-1 (ATCC®-CRL-3243), and human keratinocyte HaCaT (ATCC®-PCS-200–011) cells were used. PC-3 and H838 cells were cultured in Roswell Park Memorial Institute (RPMI)− 1640 medium (Invitrogen, Paisley, UK) mixed with 10% (v/v) foetal bovine serum (FBS, Gibco, Paisley, UK) and 1% penicillin–streptomycin (Gibco, Paisley, UK, 10,000 U/mL). U251MG and HaCaT cells were cultured in Dulbecco's modified Eagle medium (DMEM) (Sigma, St Louis, Missouri, USA) mixed with 10% (v/v) FBS and 1% penicillin–-streptomycin (10,000 U/mL). HMEC-1 cells were cultured in MCDB 131 medium (without L-glutamine, Gibco, Paisley, UK) mixed with 10 ng/mL epidermal growth factor (EGF, Thermo Fisher Scientific, Horsham, UK), 1 μg/mL hydrocortisone (Thermo Fisher Scientific, UK), 10 nM of L-glutamine (Thermo Fisher Scientific, Horsham, UK), 10% (v/v) of FBS and 1% penicillin–streptomycin (10,000 U/mL). A total of 8000 cells/well were seeded in the 96-well plates overnight.

For the peptide groups, the final concentration of the peptides ranged from 100 μM to 10 nM. The negative control and positive control groups were spiked with fresh serum-free medium containing equal amounts of PBS and 0.1% (w/v) Triton-X-100, respectively. The 96-well plate was then incubated at 37 °C with 5% CO_2. After 24 h of incubation, 10 μL of MTT solution (5 mg/mL) (Sigma, Gillingham, UK) were added to each well and incubated in a dark environment for 2 h. The solution was then removed from each well and 100 μL of DMSO was added. Finally, the plate was shaken for 10 min in a shaking incubator before detecting the OD value using a Synergy HT plate reader at λ = 570 nm. All experimental groups required three repetitions, and the experiment was repeated three times.

2.10. Haemolysis assays

Defibrinated horse erythrocytes (TCS Biosciences Ltd., Buckinghamshire, UK) were treated with different peptide solutions to assess the haemolytic activity of B1AW and its analogue, B1AW-K. Before testing, horse blood cells were washed with PBS three times. Then 50 mL of sterilised PBS was added to 2 mL of blood in a tube to make the 4% (v/v) red blood cell suspension. Next, 100 μL of peptides at different concentrations (100 μM, 50 μM, 10 μM, 5 μM, 1 μM) were incubated with 100 μL of red blood cell suspension at 37 °C for 2 h. Blood cells treated with 1% Triton-X 100 were used as a positive control and blood cells treated with PBS were used as a negative control. After incubation, 100 μL of the supernatant of each sample was transferred to a new 96-well plate and the OD value of each well was measured with a Synergy HT plate reader at an absorbance of 570 nm. The haemolysis effect (%) was calculated as follows:

$$\text{Haemolysis}(\%) = \frac{\text{A(sample)} - \text{A(negative control)}}{\text{A(positive control)} - \text{A(negative control)}} \times 100\%$$

2.11. Molecular dynamic simulation systems and parameters

To gain further insight into the structure and dynamics of B1AW and B1AW-K in the cell membrane, MD simulations were performed for all atoms. The initial structures of B1AW and B1AW-K were predicted using the PEP-FOLD server (as mentioned in 2.5). The N- and C-termini of the peptides were charged, and the lysine side chains were protonated to mimic experimental conditions. The equilibrated anionic DOPCDOPS membrane model (in a ratio of 3:1) from our previous work [24] was used to mimic the highly negatively charged cancer cell membrane. NaCl ions were added to neutralise the systems and reach the physiological state. A peptide was added to the water phase with a minimum distance of at least 2.8 nm from the membrane. All peptide-membrane systems were first energy-minimised using the steepest-descent algorithm, followed by 100 ps equilibration in NVT and 100 ps in NPT with position restraints for the protein heavy atoms. Finally, all restrictions were released for production runs with data collected every 10 ps.

Simulations were performed using the GROMACS 2021.3 package [25] with CHARMM36m force field and the TIP3P water model. Periodic boundary conditions were applied in all directions. Electrostatic interactions were calculated using particle mesh Ewald (PME) with a Coulomb cut-off of 1.2 nm, while short-range van der Waals interactions were cut-off at 1.0 nm and forced to decay smoothly to zero until 1.2 nm with the force-switch function. All hydrogen atoms were constrained. For production runs, the system temperature was regulated with the Nosé -Hoover coupling method at 310 K with separate couplings for the peptide, lipids, and solvent (water and ions) and a time constant of 1 ps. The pressure was regulated semi-isotropically with a Parrinello–Rahman thermostat at 1 bar and a time constant of 5 ps. The leap-frog algorithm was used for integrating Newton's equations of motion with a time step of 2 fs [24].

A summary of the peptide-membrane systems studied is shown in Table S1. Peptide-membrane systems were simulated four times, each with different starting velocities and two different random orientations of the peptide in the water phase. To compare the conformational change of the peptide in the membrane with that of the water solution, both B1AW and B1AW-K were simulated in a box of water molecules under physiological ionic conditions in four replicates. Therefore, there were 16 systems in total and each simulation was run for 1 μs.

2.12. Statistical analysis

All results were obtained from at least three replicates for each experiment. Data were analysed using GraphPad Prism 8.0 software. Data are presented as mean ± standard deviation (SD). Statistical significance was indicated by $p < 0.05$, based on one-way or two-way ANOVA calculated by a multiple *t* test.

3. Results

3.1. Molecular Cloning of B1AW precursor-encoding cDNA

The precursor-encoding cDNA of the novel peptide was consistently cloned from the skin secretion library of *A. wuyiensis*. Fig. 1A shows the open reading frame of the mature peptide-encoding precursor, which consisted of 71 amino acids. The signal peptide region consisted of 22 amino acids and was followed by a 23-amino acid spacer. Then, a typical putative cleavage site of the lysine-arginine residue (K-R) was present at the N-terminus, and the mature peptide consisted of 24 amino acids.

A Basic Local Alignment Search Tool (BLAST) analysis of the novel peptide, using the NCBI database, demonstrated the precursor of this peptide exhibited high sequence identity with a reported peptide, brevinin-1E from *Rana esculenta* [26], in which there were only three amino acid differences in the mature peptide region (Fig. 1B). Therefore, the newly discovered peptide was named brevinin-1-AW (B1AW, 'AW' refers to its origin).

3.2. Purification and identification of B1AW

The crude synthesised peptides were purified by reverse phase HPLC and the chromatographic fractions were collected and are shown in Fig. S1A. The mass spectra of the collected samples containing the pure peptides showed only one major species, along with a small sodium or potassium adduct, following that peak in each chromatogram. Therefore, the molecular masses of the purified peptides were confirmed (Fig. S1B).

3.3. Antimicrobial activity of B1AW and targeted peptide design

As shown in Table 1, B1AW displayed anti-bacterial activity against the three Gram-positive bacteria tested (*S. aureus, MRSA,* and *E. faecalis*), with MICs of 32 μM and MBCs from 32 to 64 μM.

As a typical member of the brevinin-1 family, B1AW showed a relatively limited antimicrobial spectrum and only had inhibitory effects on the three Gram-positive bacteria tested. According to a previous report, cationicity is the initial factor in the interaction between AMPs and cell membranes [27]. To broaden the antimicrobial spectrum of B1AW, a positively charged lysine residue (K) was used to replace glutamine (Q) at the position 15 to obtain B1AW-K. The peptide sequences are listed in Table 2. B1AW-K was synthesised and purified by reverse phase HPLC, and the chromatographic fractions were collected as shown in Fig. S1C. The mass

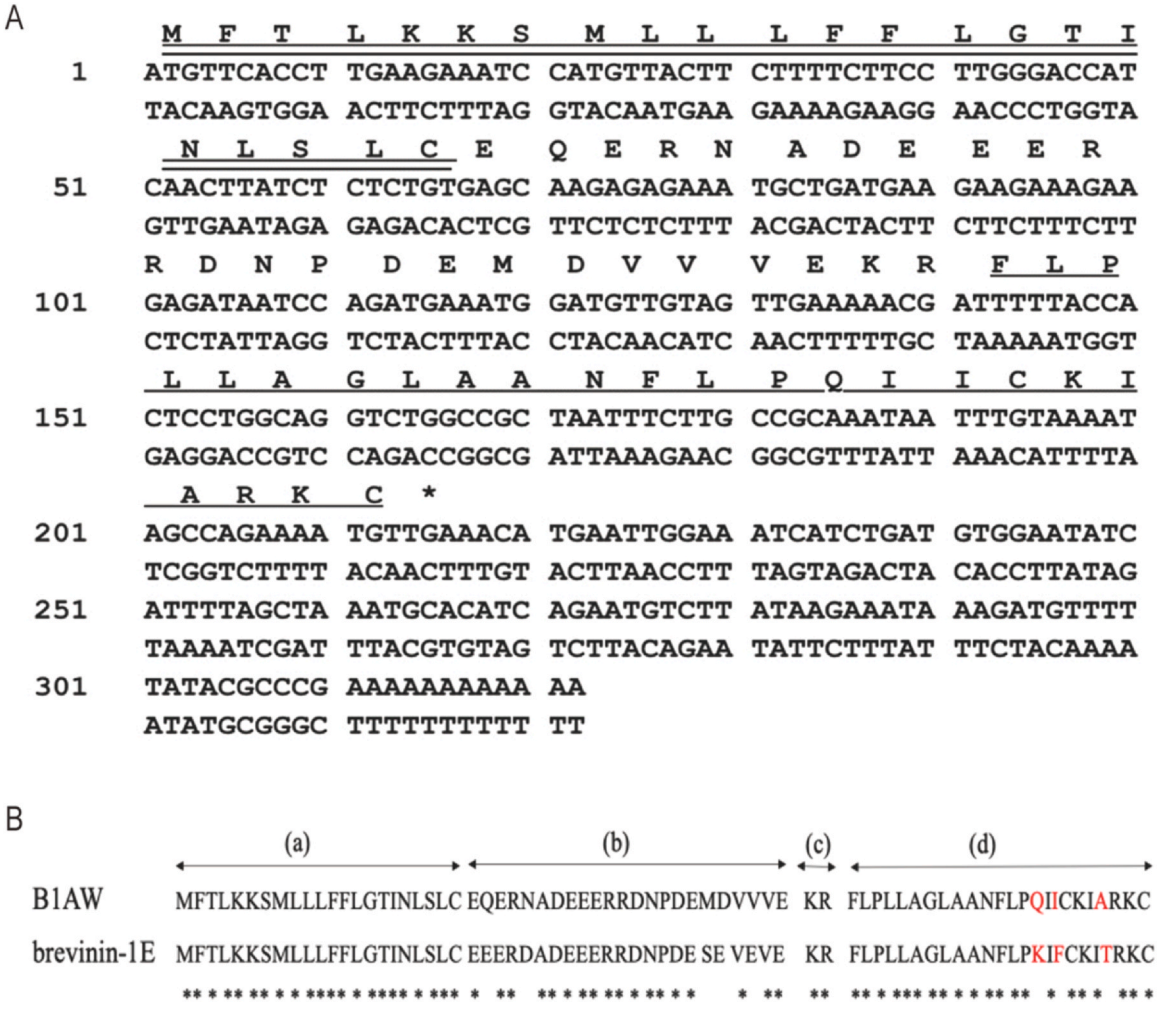

Fig. 1. (A) Alignment of the nucleotide and translated open reading frame of the cloned peptide precursor-encoding cDNA obtained from the skin secretion of *Amolops wuyiensis*. The putative signal peptide is marked with a double underline, the mature peptide is marked with a single underline, and the stop codon is marked with an asterisk. (B) The amino acid sequences of B1AW and brevinin-1E precursors. (a) signal peptide region (b) acidic spacer domain (c) enzyme cleavage site (d) mature peptide region. Identical amino acid residues are represented by asterisks (*), and the different amino acid residues in the mature peptide region, are highlighted in red.

Table 1
MICs/MBCs (μM) of B1AW and B1AW-K against different microorganisms.

Microorganisms	B1AW	B1AW-K
S. aureus (ATCC 6538)	32/32	8/8
MRSA (NCTC 12493)	32/64	8/16
E. faecalis (NCTC 12697)	32/32	16/32
E. coli (ATCC 8739)	> 512/ > 512	8/16
K. pneumoniae (ATCC 43816)	> 512/ > 512	8/16
P. aeruginosa (ATCC 9027)	> 512/ > 512	16/32
C. albicans (ATCC 10231)	> 512/ > 512	256/256

spectra of the purified B1AW-K is shown in Fig. S1D. Therefore, the molecular masses of the purified peptides were confirmed.

The introduction of the lysine (K) residue broadened the antibacterial spectrum of the parent peptide. B1AW-K showed potential to inhibit the growth of the Gram-negative bacterium, with MIC values ranging from 8 to 16 μM. Compared to B1AW, B1AW-K also had enhanced antibacterial effects against Gram-positive bacteria. The MICs/MBCs values against *S. aureus* and *MRSA* decreased 4-fold compared to those of B1AW. The MICs/MBCs against *E. faecalis* also decreased to 16 μM/32 μM. Both peptides tested had a weak potency in inhibiting the yeast growth.

3.4. Secondary structure analysis and physicochemical properties of B1AW and its analogues

The chemical structures of B1AW and B1AW-K are shown in Fig. 2A and B. The 3D models of B1AW and B1AW-K were predicted by the PEP-FOLD3 server (Fig. 2C and D). Both peptides tended to form α-helical structures. Due to the proline (P) residue in the middle of the sequence (P^{14}), the α-helical structures of B1AW and B1AW-K were twisted to form a kinked structure.

The hydrophobicity and hydrophobic moments of B1AW and B1AW-K were predicted by the online analysis tool, Heliquest (http://heliquest.ipmc.cnrs.fr/cgi-bin/ComputParamsV2.py Assessed: 2023/02/21). The parent peptide, B1AW, had a relatively higher hydrophobicity

Table 2
Peptide sequences and physiochemical properties of B1AW and B1AW-K.

Peptide name	Sequence	Net charge < z >	Hydrophobicity < H >	Hydrophobic moment < μH >	% α-helicity in 50% TFE
B1AW	FLPLLAGLAANFLPQIICKIARKC	3	0.810	0.290	33.73
B1AW-K	FLPLLAGLAANFLPKIICKIARKC	4	0.777	0.314	36.2

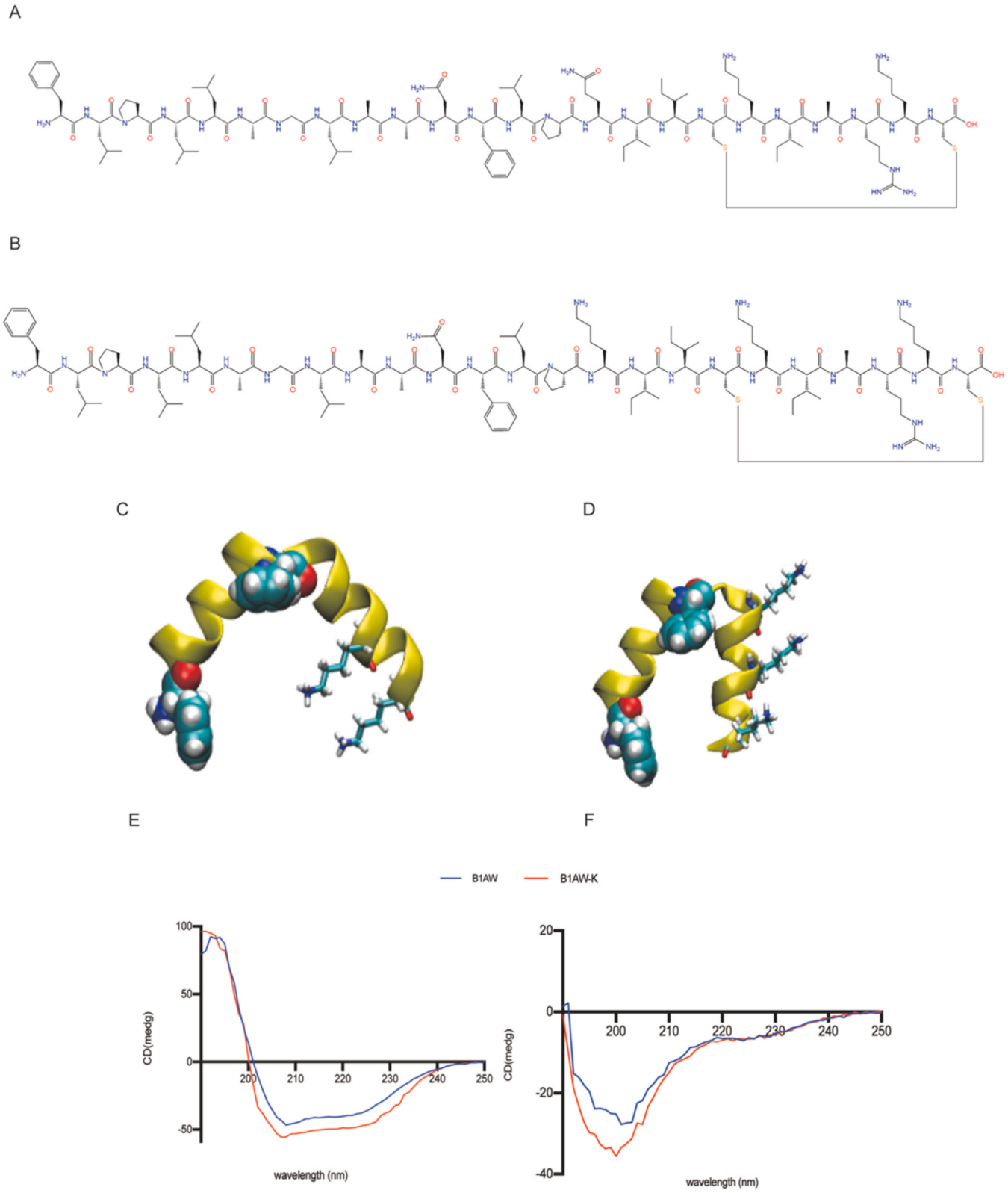

Fig. 2. (A) Chemical structure of B1AW. (B) Chemical structure of B1AW-K. (C) The 3D model predicted by the PEP-FOLD server for B1AW. (D) The 3D model predicted by the PEP-FOLD server for B1AW-K. Peptide backbones are shown in the cartoon, lysine residues as sticks, Phe^{1} and Phe^{12} as spheres. (E) Circular dichroism spectra of B1AW and B1AW-K (100 μM) in 50% TFE/NH_4AC. (F) Circular dichroism spectra of B1AW and B1AW-K (100 μM) in 10 mM NH_4AC buffer.

(0.810) and a lower hydrophobic moment (0.290). Using a lysine residue (K) to replace a glutamine residue (Q) at position 15, the hydrophobicity of B1AW-K was reduced to 0.777, and the hydrophobic moment increased to 0.314 (Table 2).

CD studies of B1AW and B1AW-K were performed in NH_4AC buffer and 50% TFE/NH_4AC buffer. CD spectra in an aqueous solution indicated the presence of random coil structures for these two peptides (Fig. 2E). In comparison, CD spectra showed that the tested

Table 3
MBICs/MBECs (μM) of B1AW and B1AW-K against the three test Gram-positive bacteria.

Bacteria strains	B1AW	B1AW-K
S. aureus (ATCC 6538)	32/ > 256	16/ > 256
MRSA (NCTC 12493)	32/ > 256	16/ > 256
E. faecalis (NCTC 12697)	64/ > 256	32/ > 256

peptides tended to form α-helix structures in 50% TFE with two negative peaks at 208 and 222 nm and a positive peak at 192–195 nm (Fig. 2 F). The CD spectra were then analysed by Webserver K2D3 http://cbdm-01.zdv.uni-mainz.de/~andrade/k2d3/; Assessed: 2023/02/21) to calculate the α-helical content of each peptide in 50% TFE. The designed analogue, B1AW-K, had a lower α-helical content (33.73%) than B1AW (36.2%).

3.5. Antibiofilm activity of B1AW and its analogues

B1AW and its lysine-modified analogue B1AW-K displayed various antimicrobial activities in MIC and MBC assays. Based on the results of antimicrobial assays, the Gram-positive bacteria, *S. aureus, MRSA, and E. faecalis,* were selected to detect the anti-biofilm activity of B1AW and B1AW-K (Table 3); Gram-negative bacteria, *E. coli*, *K. pneumoniae,* and *P. aeruginosa* were used to detect the antibiofilm activity of B1AW-K (Table 4).

The two tested peptides could inhibit the initial formation of biofilm of Gram-positive bacteria at the corresponding MBCs or two-fold of MBCs concentrations but could not eradicate the biofilm at the concentrations tested (MBECs > 256 μM).

Using a lysine residue (K) to substitute the glutamine residue (Q) at position 15, the B1AW-K MBIC against these three Gram-positive bacteria decreased to half that of B1AW. Surprisingly, at a high concentration (256 μM), B1AW-K not only inhibited the initial formation of biofilm in the corresponding MBCs, but also developed biofilm eradication effects against the Gram-negative bacteria tested.

3.6. Time-killing kinetics of B1AW and B1AW-K

The killing efficiency of B1AW and B1AW-K against *S. aureus* (ATCC 6538) was observed at concentrations corresponding to the MIC (Fig. 3A) and 2 x MIC (Fig. 3B) in 180 min. The time-killing curves indicated that at the tested concentrations, both peptides could cause the complete death of *S. aureus* in 180 min. B1AW-K could kill bacteria in 90 min at its MIC, but it only needed 60 min to kill bacteria at 2 x MIC. However, B1AW took 180 min to kill the bacteria at the MIC and at 2 x MIC. In comparison, B1AW-K had a more rapid killing kinetic ability at a concentration of both MIC and 2 x MIC.

3.7. Permeabilisation effects of B1AW and B1AW-K on the bacterial cell membrane

To investigate the antibacterial mechanism of action of peptides, a SYTOX green staining assay was conducted. Gram-positive *S. aureus* (ATCC 6538) and Gram-negative *E.coli* (ATCC 8739) bacteria, were selected as targets for this assay. Based on the results of the MIC assay, parent peptide B1AW did not show an obvious antimicrobial effect against *E.coli*, thus, it was not included in the corresponding test.

Table 4
MBICs/MBECs (μM) of B1AW-K against the three test Gram-negative bacteria.

Bacteria strains	B1AW-K
E. coli (ATCC 8739)	16/256
K. pneumoniae (ATCC 43816)	16/256
P. aeruginosa (ATCC 9027)	32/256

The effects of cell membrane permeability within 2 h, of B1AW and B1AW-K exposure against *S. aureus* and *E. coli,* were tested in their respective concentrations of MIC, 2 x MIC and 4 x MIC concentrations (Fig. 3 C). B1AW and its B1AW-K demonstrated a significant effect of membrane permeability on *S. aureus*. B1AW caused more than 60% permeabilisation on *S. aureus* at its MIC, and the permeability rate improved to nearly 100% when the concentration increased up to 2 x MIC and 4 x MIC. B1AW-K generated an almost 100% permeability rate at the concentrations tested, which did not increase as the concentration increased.

Regarding the effects of permeability on Gram-negative bacteria, B1AW-K was active on the *E. coli* membrane in a concentration-dependent relationship (Fig. 3D). B1AW-K caused an obvious membrane rupture effect on *E. coli* (the permeability rates were around 60%) at the corresponding MIC. At high concentrations (2 x MIC and 4 x MIC), B1AW-K caused nearly 70–100% permeabilisation of *E. coli*.

3.8. Antiproliferative activity of B1AW and B1AW-K

The parent peptide B1AW showed a broad-spectrum antiproliferative effect against the three tested cancer cell lines, with IC_{50} values ranging from 32.15 μM to 33.56 μM, but also showed high cytotoxicity for two human normal cell lines, HMEC-1 and HaCaT (IC_{50}: 32.96 μM and 44.09 μM, respectively) (Table 5). Using a lysine residue (K) to substitute Q^{15}, B1AW-K showed an additional enhanced ability to inhibit the growth of all cell lines tested. The antiproliferative effects on the three cancer cell lines were revealed after treatment with 10^{-5} M B1AW-K; The cell viabilities of these cancer cell lines were less than 20% (Fig. 4 A). Furthermore, the antiproliferative effects of B1AW-K in two normal human cell lines were also acceptable, cell survival rates were higher than 70% with the treatment of 10 μM of B1AW-K (Fig. 4B).

3.9. Haemolytic activity of B1AW and its analogues

The results of the haemolysis assay showed that B1AW and B1AW-K had intense haemolytic activity even at a low concentration (5 μM), with a haemolytic rate of more than 20% (Fig. 5). After the introduction of a lysine residue, B1AW-K processed an even lower HC50 value (10.6 μM) than the parent peptide (Table 6).

3.10. Simulation of peptide adsorption onto the anionic membrane

To investigate the differences in structure and dynamics between B1AW and B1AW-K during the membrane adsorption process, equilibrium MD simulations were performed. The membrane model was a 3:1 mixture of neutral DOPC lipids and negative DOPS lipids to mimic the anionic environment of the cancer cell membrane. The time evolution of the distance of the peptide (centre of mass) to the bilayer headgroup is shown in Fig. 6 A and 6B. B1AW-K exerted a stronger attraction to the membrane, due to the increase in the net charge of the peptide with the N-terminal K^{15} mutation. The initial binding of B1AW-K to the anionic membrane was observed in less than 75 ns in the four simulation replicates (S1 to S4), compared to 350 ns for B1AW, which was on average six times faster for B1AW-K than for B1AW to bind to the membrane (See Supplymentary Table S2). The time it took the peptide to adsorb in the membrane phosphate headgroup layer varied from 100 to 650 ns for B1AW and 300–900 ns for B1AW-K. Note that S3 of B1AW-K remained attached to the membrane surface until the end of the simulation.

Visual inspection of the simulations showed that the initial contact between the two peptides and the membrane began with positively charged lysine residues at the C-terminal segment of the

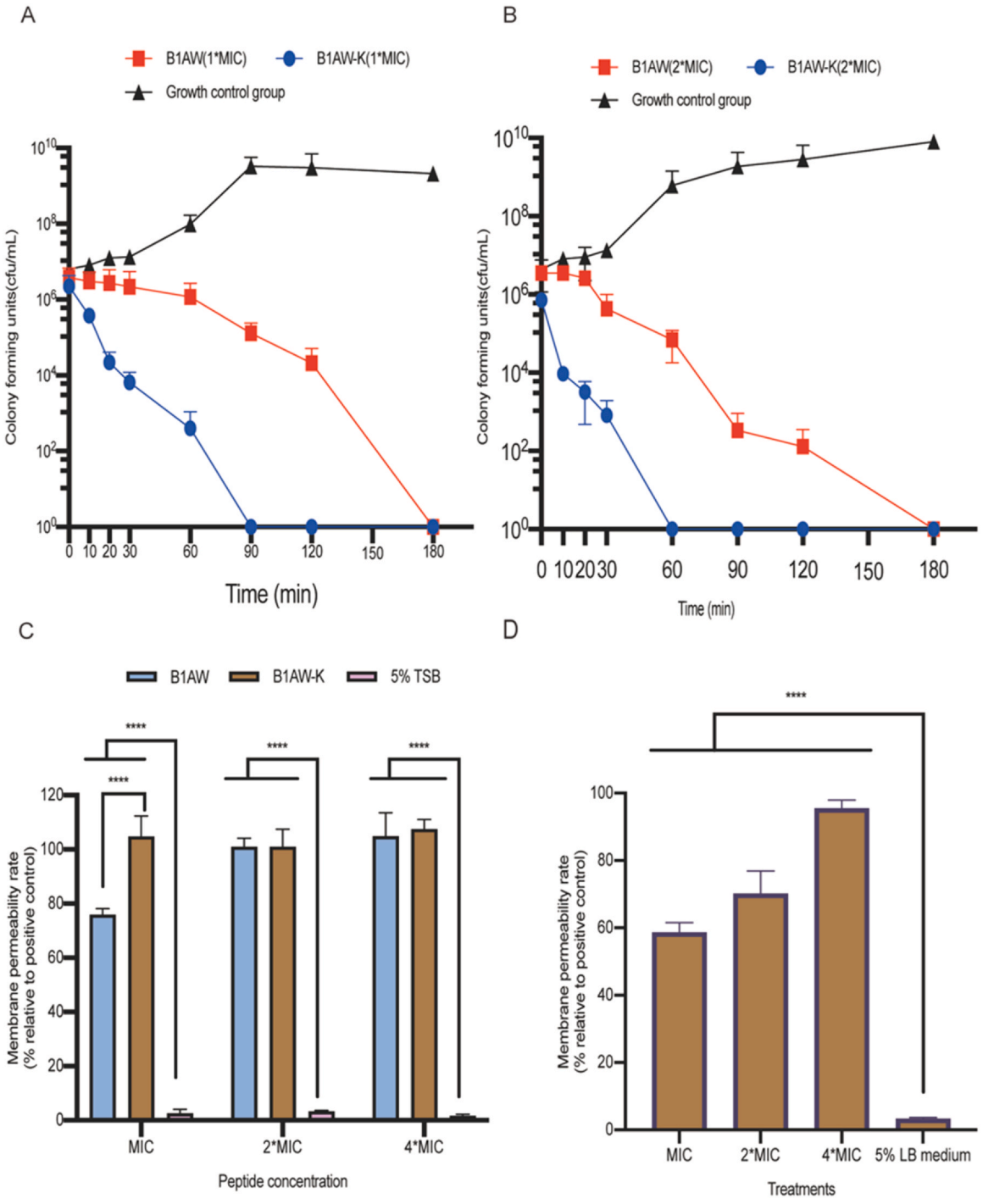

Fig. 3. (A) Time-killing curves of *S. aureus* killed by B1AW and B1AW-K at their corresponding MICs. (B) Time-killing curves of *S. aureus* killed by B1AW and B1AW-K at their corresponding 2 ×MICs. Bacteria with no peptide treatment were used as growth control. The error bars indicate the *SD* of nine replicates. (C) The membrane permeability effects on *S. aureus* at concentrations of 1 ×MIC, 2 ×MIC and 4 ×MIC of peptide treatments. (D) The membrane permeability effects on *E.coli* at concentrations of 1 ×MIC, 2 ×MIC and 4 ×MIC of peptide treatments. The error bars represent the *SDs* of nine replicates. Significant differences are indicated as $^{****}p < 0.0001$.

Table 5
The IC_{50} values (μM) of B1AW and B1AW-K against five tested cancer cell lines.

Peptide	PC-3	H838	U251MG	HMEC-1	HaCaT
B1AW	33.46	32.15	33.56	32.96	44.09
B1AW-K	4.283	5.15	3.860	26.45	20.53

peptide chain. Upon contact, B1AW entered the membrane with its N-terminal segment, which remained as a long (ca. 10–12 residues) stable helix until the end of the simulation time, except in one case (S4) where a break was seen in the middle of the chain (see Fig. 6 C, Final snapshots of B1AW). In contrast, for B1AW-K, only parts of the chain, from the N-terminal half (S1, S4), or the C-terminal half (S2, S3) of the peptide remained helical and the middle segment (ca. 5 residues) was fully unfolded (see Fig. 6D, Final snapshots of B1AW-K).

To elucidate the structures of the peptides in the membrane-adsorbed state, we analysed the secondary structure of the peptide using the DSSP programme. As shown in Fig. 6E and F (also in Table 7), the two peptides assumed very different structures, which

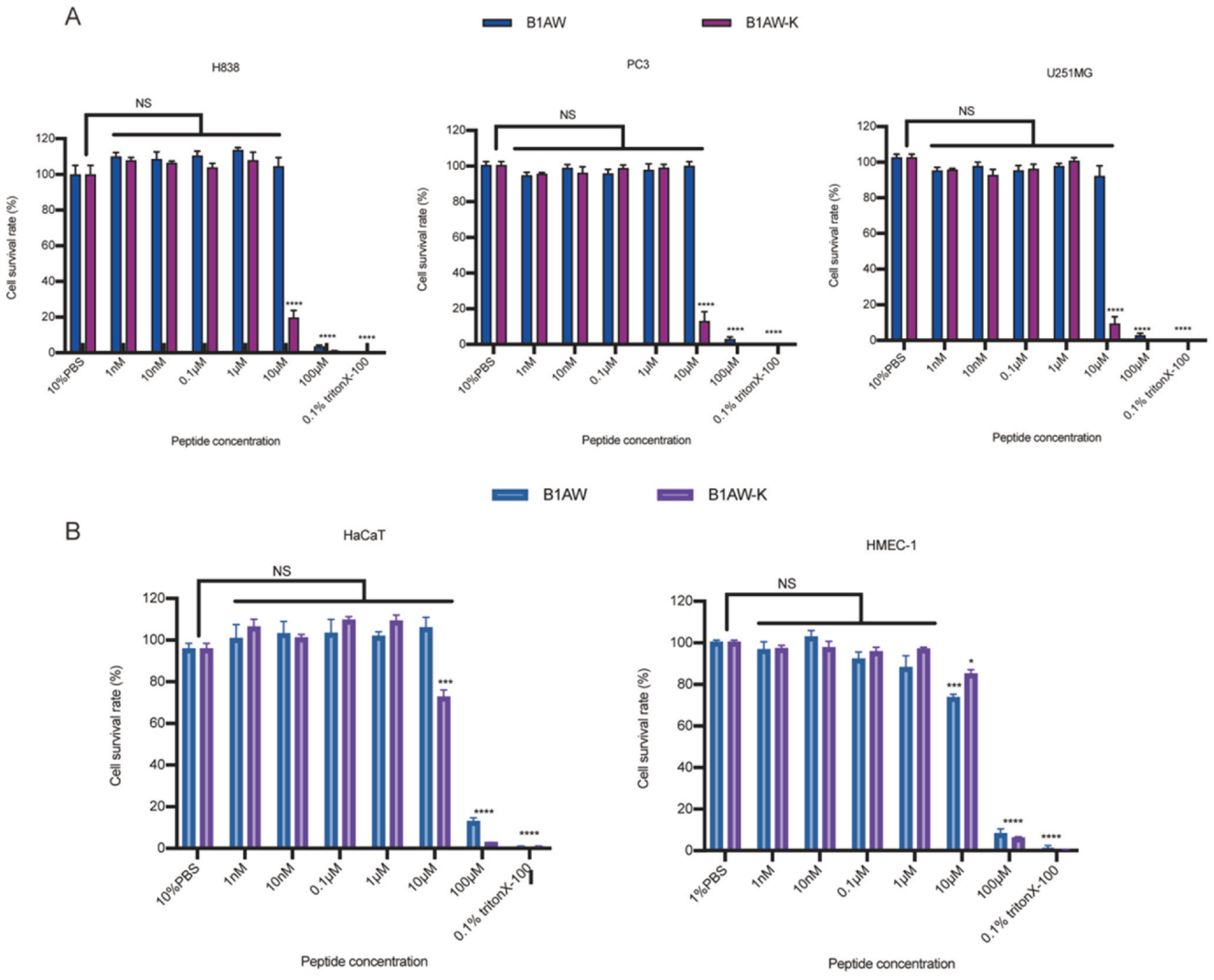

Fig. 4. Antiproliferative activity of B1AW and B1AW-K in the range of 100 μM to 1 nM after 24 h treatment. (A) B1AW and B1AW-K activity against three tested cancer cell lines. (B) B1AW and B1AW-K against two human normal cell lines. Panels display the cell viability (%) on five tested cell lines. The relative serum-free medium with 0.1% Triton X-100 was set as the positive control group, and the relative serum-free medium with 1% PBS was selected as the negative control group. The error bar indicates the *SD* of nine replicates. 'NS' means there was no significant difference between the treatment and negative control groups. Significant differences are indicated as $^{****}p < 0.0001$, $^{***}p < 0.001$, $^{*}p < 0.05$.

is in agreement with our visual observations. B1AW had an average fraction of 68.77% of the chain forming a helix. Additionally, some residues at the C-terminus unfolded to keep the charged amino acids at the hydrophilic headgroup layer of the membrane. Conversely, for B1AW-K only 45.71% of the chain was a helix, while the remaining 49% of the chain was a random coil.

The middle coil segment in B1AW-K allowed greater flexibility and dynamics of the peptide in the membrane, leading to increased disruption of the membrane. To provide evidence supporting these properties, the disorderness of the bilayer was measured using the lipid order parameters as a function of the carbon number in the acyl chain of the lipid. As shown in Fig. S3, when the peptide was inserted deeper into the bilayer core, the order parameters of the lipid tails were reduced. In general, the reduction in the lipid structure was obvious when a peptide was inserted deep within the membrane. In particular, slightly lower lipid order parameters were measured in S4 of B1AW-K compared to S4 of B1AW. Unfortunately, we did not observe deeper penetration of the peptide into the membrane even with extended simulation time (B1AW-K S4 up to 1500 ns).

It is well-known that some AMPs do not achieve a stable conformation in solution. To determine whether this was the case for B1AW and B1AW-K, the peptides were also simulated in a box of water molecules. In the water phase, B1AW-K exhibited larger conformational changes than B1AW, as revealed by the "spikes" in the time-dependent RMSD plot of B1AW-K, which were absent for B1AW (Supplementary Fig. S4). DSSP analysis revealed that B1AW had a higher proportion of helix compared to B1AW-K. Similar to what was observed for the membrane assays, the N-terminal half of B1AW-K assumed no stable structure, while the C-terminal half had a higher occurrence of the helix.

Taken together, our MD results suggest that the introduction of a charged residue in the middle of the chain leads to a more disordered structure of the peptide B1AW-K and its increased flexibility in both the water solution and the membrane. We observed a faster binding of B1AW-K to the anionic membrane and a deeper penetration of the peptide into the hydrophobic core, resulting in a decrease in lipid order.

4. Discussion

Amphibian skin secretion-derived peptides are now considered alternative antimicrobial agents because of their wide-spectrum of

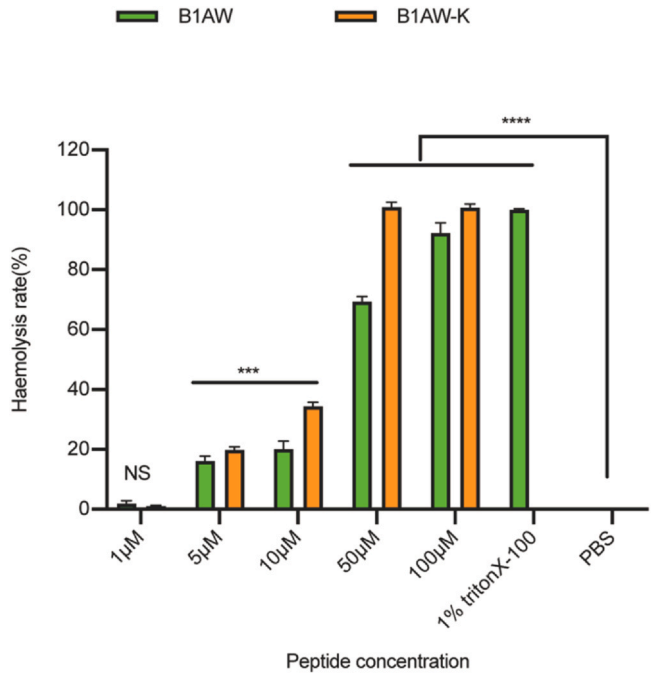

Fig. 5. The haemolytic activity of B1AW and B1AW-K towards horse red blood cells. 0.1% Triton X-100 buffer was used to treat the positive control group, and PBS was used to treat the negative control group. The error bar indicates the *SD* of nine replicate. 'NS' means there was no significant difference between the treatment and negative control groups. Significant differences are indicated as $^{****}p < 0.0001$, $^{***}p < 0.001$.

Table 6
The HC_{50} (μM) values of B1AW and B1AW-K towards horse red blood cells.

Peptides	HC_{50}
B1AW	23.96
B1AW-K	10.6

antimicrobial activities and the low potential for drug resistance. Due to the rapid development of antibiotic resistance in recent years, the application of AMPs as has been proposed [28–31] and brevinin peptides are typical examples. In this study, a new brevinin peptide was isolated from *Amolops wuyiensis* and named B1AW. B1AW showed potency in inhibiting the growth of Gram-positive bacteria at 32 μM. Contrary to previous reports [32,33], B1AW did not show broad-spectrum antimicrobial activity coupled with excess haemolytic activity. Therefore, it was necessary to optimise its bioactivities through rational modification.

Generally, the outer membrane of Gram-negative bacteria, with their high concentration of negatively charged lipopolysaccharide, provides them with a more complex membrane than that of Gram-positive bacteria [34]. This may explain why B1AW had no effect on the growth of Gram-negative bacteria. To improve the selectivity of the peptide against Gram-negative bacteria, a lysine (K) residue was used to substitute the glutamine (Q) residue at the position 15. This modification was based on the theory that a lysine residue on the hydrophobic face could prevalently maintain peptides as unstructured monomers and could achieve the α-helical structure under hydrophobic conditions, allowing them to interact with the membrane of Gram-negative bacteria [35,36]. B1AW-K was able to kill the Gram-negative bacterium, *E.coli*. These results proved that positively charged residues on the non-polar face of the helical conformation can modulate Gram-negative bacterial specificity.

For the AMP action mode, the widely accepted theory is the AMP-membrane interaction, including the Barrel-Stave model, the Carpet model, and the Toroidal pore model [37,38]. Briefly, cationic AMPs were initially attracted by the anionic cell membrane and processed the stable α-helical structure. The amphiphilicity of AMPs promotes peptides to form pores or align parallel to the surface of the cell membrane and then cause disruption of the cell membrane[39,40]. B1AW and its modified B1AW-K also caused membrane permeabilisation in the tested bacterial cell membrane. The introduction of a lysine residue further enhanced this effect. B1AW-K caused almost 100% damage to the *S. aureus* cell membrane at its MIC concentration.

From a different perspective, significant research has shown that bacteria play a crucial role in cancer progression [41]. For example, *Helicobacter pylori* is considered a bone-fide carcinogen by the International Agency for Research on Cancer, and causes gastric cancer in 1–3% of colonised individuals [42,43]. Thus, regulation of the unbalanced microbiome may be an effective way to interfere with the progression of certain cancers. Dual-effect AMPs might be ideal candidates in cancer therapy. Compared to other reported brevinins (e.g. brevinin 1GHa, brevinin 1GHb, brevinin 1GHc, and brevinin 1E) [44], B1AW-K exhibited superior antiproliferative activity against the three cancer cell lines tested. This phenomenon was inseparable from the enhanced cationicity. Cancer cells have higher levels of negatively charged phosphatidylserine and O-glycosylated mucin on their surfaces than normal cells, and B1AW-K with enhanced cationicity was better able to interact with negatively charged cancer cell membranes [45].

To define the selectivity and membrane binding ability of peptides from a molecular standpoint, we simulated B1AW and B1AW-K in two membrane types, DOPC (representing the normal mammalian cell membrane) and DOPC/DOPS (representing the anionic cancer cell membrane), and in bulk [24]. Both these peptides had a low frequency of adsorption in DOPC. Furthermore, B1AW-K approached DOPC/DOPS more rapidly than B1AW, which was at least six times faster. These findings confirmed the contribution of a lysine residue in the interaction between peptides and cell membranes. In our simulations, the introduction of an extra lysine residue caused a change in the structure once the peptides reached the membrane environment. B1AW entered the membrane with its N-terminal segment, which prolonged the stability of the helix. In contrast, in B1AW-K, only parts of the chain, from the N-terminal half (S1, S4), or the C-terminal half (S3), or both (S2) of the peptide, remained helical and the middle segment fully unfolded. The middle coil segment in B1AW-K allowed greater flexibility and dynamics of the peptide in the membrane, leading to stronger membrane disruption. However, the cytotoxicity of brevinins is undeniable, and this also applied to B1AW and B1AW-K [46].

Brevinin-1E is one of the brevinin-1 peptides with potent antimicrobial and haemolytic activities. According to the results of the MIC assays, brevinin-1E can inhibit the growth of the Gram-positive and Gram-negative bacteria tested at low concentrations (from 3.12 to 6.25 μg/mL). However, the HD_{50} value of brevinin-1E was only 1.1 μg/mL, which indicated a strong haemolytic activity [47]. Furthermore, *Limnonectes fujianensis* Brevinvin (LFB) is a brevinin-like peptide with considerable antiproliferative activity against a series of cancer cell lines, including H460, HCT116, and MB435 cells. However, the high haemolytic activity of LFB at a concentration of 16 mg/L prevents its excellent antiproliferative activity from being utilised [48].

High haemolytic activity is also the bottleneck in the use of B1AW and B1AW-K. With the overall promotion of both antimicrobial and antiproliferative activities, the haemolytic activity of B1AW-K was almost twice than that of B1AW. Previous studies have shown that the decrease in hydrophobicity directly contributes to a reduced haemolytic activity [49,50]. The hydrophobic part of the brevinin-1 peptides is mainly concentrated in the N-terminal FLP region [12,51]. B1AW-K possesses an additional 'FLP' domain in its sequence, which is not a

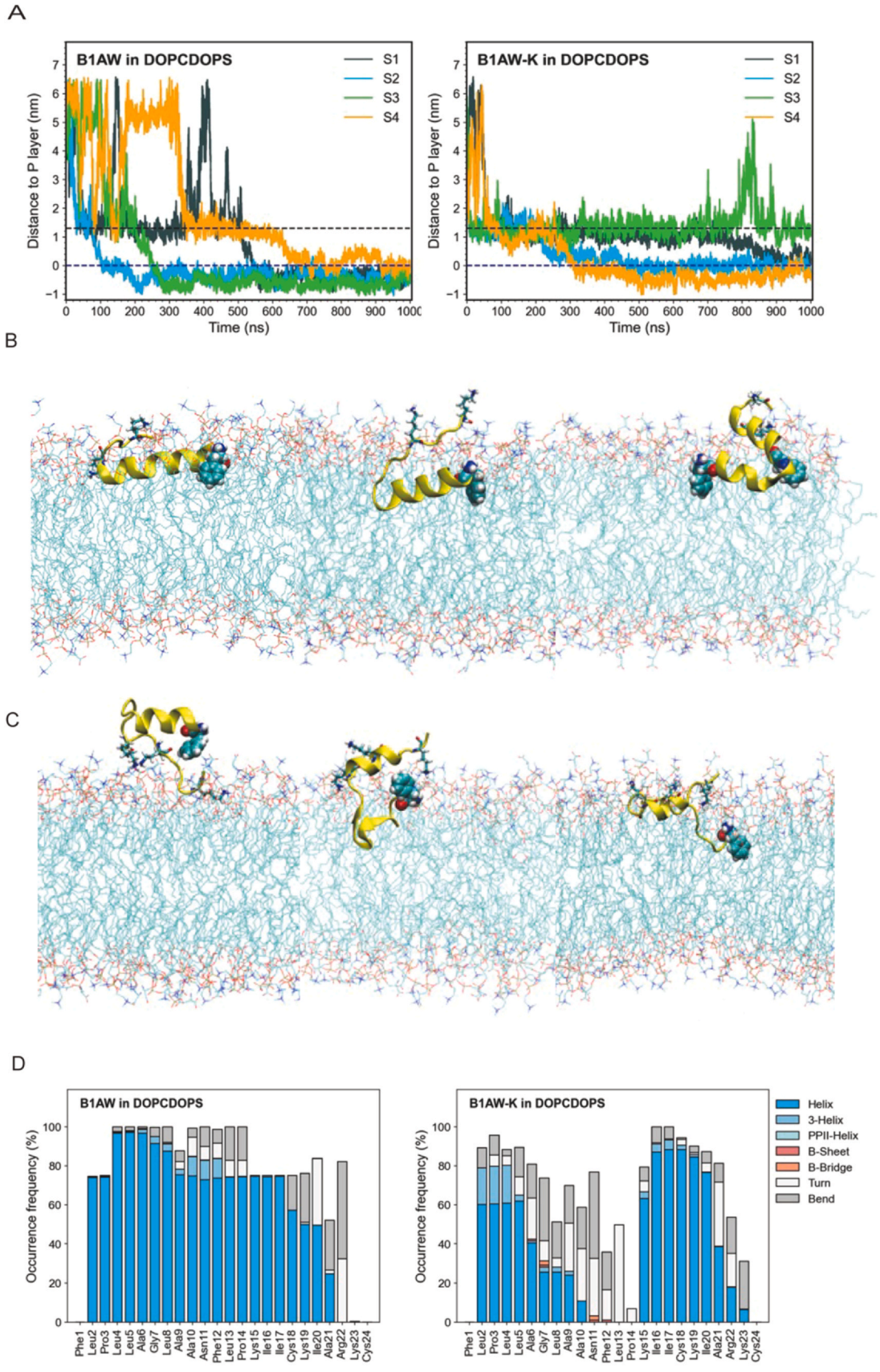

(caption on next page)

Fig. 6. Simulation of B1AW and B1AW-K adsorption onto the anionic membrane (A) B1AW and B1AW-K adsorption processes demonstrated by time evolution of the distance between the centre of mass of peptide and the phosphate headgroup layer of the membrane (four simulation repeats S1 to S4). (B) Selected final snapshots of B1AW in membrane (from left to right: S1, S2, S4). (C) Selected final snapshots of B1AW-K in the membrane (from left to right: S3, S1, S4). Final snapshots (1 μs) of adsorbed peptide in the membrane. The peptide chain is displayed in the yellow cartoon: the first residue (Phe1) is drawn as spheres, the lysine residues as sticks. The bilayer is drawn as lines. (D) Secondary structure frequency of peptides in the membrane adsorbed state. The peptide's secondary structure was computed using the DSSP program and the GROMACS tool do DSSP on the last 200 ns trajectories. The recognized secondary structures include three types of helixes (An alpha helix, 3-turn helix, 5-turn helix), two types of beta (beta-sheet, beta-bridge), hydrogen-bonded turn, bend (regions with high curvature). For residues where SS was not recognized, they were considered as coil, and not displayed in the plot. Occurrence frequency was averaged over the last 200 ns simulation trajectory of four repeats.

Table 7
Summary of the system properties of B1AW and B1AW-K in 1 μs waterbox and membrane simulations.

Peptide	Environment	No. of adsorbed cases	Adsorption time range	Adsorption depth (last 100 ns)	Average peptide RMSD ± SE (nm)	Percentage of SS in peptide+		
						Helix	Beta	Coil
B1AW	WATERBOX	–	–	–	0.515 ± 0.015	53.81	0.71	42.50
B1AW-K	WATERBOX	–	–	–	0.436 ± 0.054	36.19	4.66	27.86
B1AW	DOPCDOPS	4	100–600 ns	-0.318 ± 0.147	0.451 ± 0.049	68.77	0.00	30.35
B1AW-K	DOPCDOPS	4	< 100 ns	0.451 ± 0.380	0.386 ± 0.016	45.71	0.37	49.31

– No data
+ SS was calculated for the peptide chain from residue 2 to residue 23 using the last 200 ns of simulations, i.e., excluding the first and last residues, to which were not assigned SS by DSSP.

structural feature, but has often been detected in other brevinin-1 peptides, usually in the middle of the sequence [14].

To reduce haemolytic activity, we also designed two N-terminally truncated products (Table S3). The highly hydrophobic first 'FLP' motif was deleted to obtain B1AW-K21, and the second 'FLP' motif in the middle of the sequence was retained. For B1AW-K13, the sequence before the second FLP motif (FLPLLAGL) was truncated, keeping the FLP motif at the N-terminus of the new peptide. Unfortunately, although the haemolytic activities of the modified analogues (Table S4), B1AW-K21 and B1AW-K13 were markedly reduced compared to those of B1AW-K, their antimicrobial activities against the seven microorganisms tested also strongly decreased (Table S5).

To some extent, the bioactivities of brevinvins include cytotoxicity; finding the balance between bioactivities and cytotoxicity is a long-term concern for scientists. In addition to identifying new brevinins, researchers should focus more on exploring the endogenous structure-function relationship of revinine peptides and optimising their bioactivities. For example, Kumari and his colleagues shifted the Rana box of revinine 1E from the C-terminus to a central position. The designed analogue had comparable anti-bacterial activity to the parent peptide [52]. Furthermore, the linearisation of revinine peptides may reduce haemolysis [47]. These modifications may also be used to explore the best standard of B1AW-K bioactivity in the future.

5. Conclusions

A new amphibian skin-derived peptide, B1AW, was identified. *In vitro* bioassays demonstrated its antimicrobial activity against Gram-positive bacteria and antiproliferative activity on cancer cells. By introducing a lysine modification, B1AW-K showed broad-spectrum antibacterial, potent biofilm eradicative activity, and impressive anticancer activities. Analysis of MD simulation showed a higher selectivity and faster attraction of B1AW-K to cancer cell membranes as the introduction of the lysine residue led to a more disordered structure of the peptide and gave the peptide greater flexibility and dynamics to cause the membrane permeability effect. Although accompanied by certain haemolytic activity, B1AW-K could be used as a guide for the development of new antimicrobial and anticancer drug prototypes and deserves further comprehensive study.

CRediT authorship contribution statement

Haixin Qin: Investigation, Methodology, Formal analysis, Software, Visualization, Writing – original draft preparation. **Weimin Zuo and Lilin Ge:** Investigation, Methodology, Software, Visualization. **Lei Wang, Xiaoling Chen, Chengbang Ma, Shirley W. I. Siu:** Formal analysis, Software, Visualization. **Zhijian Cao:** Methodology, Formal analysis, Data curation, Visualization. **Tianbao Chen, Mei Zhou, Hang Fai Kwok:** Conceptualization, Supervision, Formal analysis, Visualization, Writing – review & editing.

Declaration of Competing Interest

The authors declare that they have no known competing financial interests or personal relationships that could have appeared to influence the work reported in this paper.

Acknowledgements

This research was funded by the Science and Technology Development Fund of Macau S.A.R. (FDCT) (file no. 0010/2021/AFJ) and the National Science Fund of China (grant no. 32161160303). H.Q. was in receipt of a postdoctoral fellowship from the FDCT. W.Z. were in receipt of a Ph.D. Assistantship from the Faculty of Health Sciences (FHS) University of Macau (UM). The authors would like to thank the Proteomics, Metabolomics & Drug Development Core at FHS UM for advising on the circular dichroism experiment.

Appendix A. Supporting information

Supplementary data associated with this article can be found in the online version at doi:10.1016/j.csbj.2023.05.006.

References

[1] Barra D, Simmaco M. Amphibian skin: a promising resource for antimicrobial peptides. Trends Biotechnol 1995;13:205–9.
[2] Qi J, Zulfiker AHM, Li C, et al. The development of toad toxins as potential therapeutic agents. Toxins 2018;10:336.
[3] Kapoor VK. Natural toxins and their therapeutic potential. Indian J Exp Biol 2010;48:228–37.
[4] Pei X, Gong Z, Wu Q, et al. Characterisation of a novel peptide, Brevinin-1H, from the skin secretion of Amolops hainanensis and rational design of several analogues. Chem Biol Drug Des 2021;97:273–82.
[5] Martinez JL. General principles of antibiotic resistance in bacteria. Drug Discov Today Technol 2014;11:33–9.
[6] Ciumac D, Gong H, Hu X, et al. Membrane targeting cationic antimicrobial peptides. J Colloid Interface Sci 2019;537:163–85.
[7] McMillan KAM, Coombs MRP. Review: examining the natural role of amphibian antimicrobial peptide magainin. Molecules 2020;25:5436.
[8] Andersson DI, Hughes D, Kubicek-Sutherland JZ. Mechanisms and consequences of bacterial resistance to antimicrobial peptides. Drug Resist Updat 2016;26:43–57.

[9] Huang Y, Huang J, Chen Y. Alpha-helical cationic antimicrobial peptides: relationships of structure and function. Protein Cell 2010;1:143–52.
[10] Konwar AN, Hazarika SN, Bharadwaj P, et al. Emerging Non-Traditional Approaches to Combat Antibiotic Resistance. Curr Microbiol 2022;79:330.
[11] Ongey EL, Pflugmacher S, Neubauer P. Bioinspired designs, molecular premise and tools for evaluating the ecological importance of antimicrobial peptides. Pharmaceuticals 2018;11:68.
[12] Savelyeva A, Ghavami S, Davoodpour P, et al. An overview of Brevinin superfamily: structure, function and clinical perspectives. Adv Exp Med Biol 2014;818:197–212.
[13] Novkovic M, Simunic J, Bojovic V, et al. DADP: the database of anuran defense peptides. Bioinformatics 2012;28:1406–7.
[14] He H, Chen Y, Ye Z, et al. Modification and targeted design of N-terminal truncates derived from brevinin with improved therapeutic efficacy. Biology 2020;9.
[15] Morikawa N, Hagiwara K, Nakajima T. Brevinin-1 and -2, unique antimicrobial peptides from the skin of the frog, Rana brevipoda porsa. Biochem Biophys Res Commun 1992;189:184–90.
[16] Mechlia MB, Belaid A, Castel G, et al. Dermaseptins as potential antirabies compounds. Vaccine 2019;37:4694–700.
[17] Nicolas P, El Amri C. The dermaseptin superfamily: a gene-based combinatorial library of antimicrobial peptides. Biochim Biophys Acta 1788;2009:1537–50.
[18] Strandberg E, Killian JA. Snorkeling of lysine side chains in transmembrane helices: how easy can it get? FEBS Lett 2003;544:69–73.
[19] Avitabile C, Netti F, Orefice G, et al. Design, structural and functional characterization of a Temporin-1b analog active against Gram-negative bacteria. Biochim Biophys Acta 1830;2013:3767–75.
[20] Wu Y, Shi D, Chen X, et al. A novel bradykinin-related peptide, RVA-Thr(6)-BK, from the skin secretion of the hejiang frog; ordorrana hejiangensis: effects of mammalian isolated smooth muscle. Toxins 2019;11:376.
[21] Qin H, Fang H, Chen X, et al. Exploration of the structure-function relationships of a novel frog skin secretion-derived bioactive peptide, t-DPH1, through use of rational design, cationicity enhancement and in vitro studies. Antibiotics 2021;10:1529.
[22] Lamiable A, Thevenet P, Rey J, et al. PEP-FOLD3: faster de novo structure prediction for linear peptides in solution and in complex. Nucleic Acids Res 2016;44:W449–54.
[23] Andrews JM. Determination of minimum inhibitory concentrations. J Antimicrob Chemother 2001;48(Suppl 1):5–16.
[24] Ma R, Wong SW, Ge L, et al. In Vitro and MD simulation study to explore physicochemical parameters for antibacterial peptide to become potent anticancer peptide. Mol Ther Oncolytics 2020;16:7–19.
[25] Abraham MJ, Murtola T, Schulz R, et al. GROMACS: high performance molecular simulations through multi-level parallelism from laptops to supercomputers. SoftwareX 2015;1–2:19–25.
[26] Simmaco M, Mignogna G, Barra D, et al. Antimicrobial peptides from skin secretions of Rana esculenta. Molecular cloning of cDNAs encoding esculentin and brevinins and isolation of new active peptides. J Biol Chem 1994;269:11956–61.
[27] Wiradharma N, Sng MY, Khan M, et al. Rationally designed alpha-helical broad-spectrum antimicrobial peptides with idealized facial amphiphilicity. Macromol Rapid Commun 2013;34:74–80.
[28] Mukhopadhyay S, Bharath Prasad AS, Mehta CH, et al. Antimicrobial peptide polymers: no escape to ESKAPE pathogens-a review. World J Microbiol Biotechnol 2020;36:131.
[29] Nguyen LT, Haney EF, Vogel HJ. The expanding scope of antimicrobial peptide structures and their modes of action. Trends Biotechnol 2011;29:464–72.
[30] Mulani MS, Kamble EE, Kumkar SN, et al. Emerging strategies to combat ESKAPE pathogens in the era of antimicrobial resistance: a review. Front Microbiol 2019;10:539.
[31] Pfalzgraff A, Brandenburg K, Weindl G. Antimicrobial peptides and their therapeutic potential for bacterial skin infections and wounds. Front Pharmacol 2018;9:281.
[32] Thomas P, Kumar TV, Reshmy V, et al. A mini review on the antimicrobial peptides isolated from the genus Hylarana (Amphibia: Anura) with a proposed nomenclature for amphibian skin peptides. Mol Biol Rep 2012;39:6943–7.
[33] Reshmy V, Preeji V, Parvin A, et al. Three novel antimicrobial peptides from the skin of the Indian bronzed frog Hylarana temporalis (Anura: Ranidae). J Pept Sci 2011;17:342–7.
[34] Ramachandran G. Gram-positive and gram-negative bacterial toxins in sepsis: a brief review. Virulence 2014;5:213–8.
[35] Du Q, Hou X, Ge L, et al. Cationicity-enhanced analogues of the antimicrobial peptides, AcrAP1 and AcrAP2, from the venom of the scorpion, Androctonus crassicauda, display potent growth modulation effects on human cancer cell lines. Int J Biol Sci 2014;10:1097–107.
[36] Epand RM, Epand RF. Bacterial membrane lipids in the action of antimicrobial agents. J Pept Sci 2011;17:298–305.
[37] Liang Y, Zhang X, Yuan Y, et al. Role and modulation of the secondary structure of antimicrobial peptides to improve selectivity. Biomater Sci 2020;8:6858–66.
[38] Brogden KA. Antimicrobial peptides: pore formers or metabolic inhibitors in bacteria? Nat Rev Microbiol 2005;3:238–50.
[39] Shai Y. Molecular recognition between membrane-spanning polypeptides. Trends Biochem Sci 1995;20:460–4.
[40] Strahilevitz J, Mor A, Nicolas P, et al. Spectrum of antimicrobial activity and assembly of dermaseptin-b and its precursor form in phospholipid membranes. Biochemistry 1994;33:10951–60.
[41] Kozlov M. Do fungi lurking inside cancers speed their growth? Nature 2022.
[42] Pevsner-Fischer M, Tuganbaev T, Meijer M, et al. Role of the microbiome in non-gastrointestinal cancers. World J Clin Oncol 2016;7:200–13.
[43] Fox JG, Wang TC. Inflammation, atrophy, and gastric cancer. J Clin Investig. 2007;117:60–9.
[44] Chen Q, Cheng P, Ma C, et al. Evaluating the bioactivity of a novel broad-spectrum antimicrobial peptide brevinin-1GHa from the frog skin secretion of hylarana guentheri and its analogues. Toxins 2018;10:413.
[45] Bai B, Hou X, Wang L, et al. Feleucins: novel bombinin precursor-encoded nonapeptide amides from the skin secretion of Bombina variegata. Biomed Res Int 2014;2014:671362.
[46] Hossain MA, Guilhaudis L, Sonnevend A, et al. Synthesis, conformational analysis and biological properties of a dicarba derivative of the antimicrobial peptide, brevinin-1BYa. Eur Biophys J 2011;40:555–64.
[47] Kwon MY, Hong SY, Lee KH. Structure-activity analysis of brevinin 1E amide, an antimicrobial peptide from Rana esculenta. Biochim Biophys Acta 1998;1387:239–48.
[48] Li B, Lyu P, Xie S, et al. LFB: a novel antimicrobial brevinin-like peptide from the skin secretion of the fujian large headed frog, limnonectes fujianensi. Biomolecules 2019;9:242.
[49] Liang D, Li H, Xu X, et al. Design, screening and antimicrobial activity of novel peptides against Streptococcus mutans. Nan Fang Yi Ke Da Xue Xue Bao 2019;39:823–9.
[50] Liu Y, Xia X, Xu L, et al. Design of hybrid beta-hairpin peptides with enhanced cell specificity and potent anti-inflammatory activity. Biomaterials 2013;34:237–50.
[51] Chen G, Miao Y, Ma C, et al. Brevinin-2GHk from sylvirana guentheri and the design of truncated analogs exhibiting the enhancement of antimicrobial activity. Antibiotics 2020;9:85.
[52] Kumari VK, Nagaraj R. Structure-function studies on the amphibian peptide brevinin 1E: translocating the cationic segment from the C-terminal end to a central position favors selective antibacterial activity. J Pept Res 2001;58:433–41.